Enhanced Heat Rejection of Microscale Geometries in Convective Flow Boiling Evaporators

L M Safford Smith[1], W J Connacher[1,2], J C Cheng[1,3] and A P Pisano[4]

[1] Department of Mechanical Engineering, University of California, Berkeley, 5101 Etchevery Hall, Berkeley, CA , USA 94720-1774
[2] Department of Physics, University of California, Berkeley, USA
[3] Department of Electrical Engineering, University of California, Berkeley, USA
[4] Professor of ME and ECE, Dean of Engineering, University of California, San Diego, 9500 Gilman Drive, La Jolla, CA, USA 92093-0403

E-mail: saffordl@berkeley.edu

Abstract. Four surfaces have been designed, fabricated and tested under convective flow boiling (CFB) conditions in an open loop configuration. They contain features in the 10 micron range and were tested with flow velocities under 3 mm/s. To accomplish these flow rates, this work utilizes a constant pressure potential driving flow, instead of the constant flow rate imposed with a syringe pump. This limited device flooding. The evaporation surfaces were tested to the point of dry-out at three different pressure potentials: 150, 650, and 1150 Pa, across a range of powers from 25 W/cm^2 to 50 W/cm^2. Temperature data was collected from an IR Camera and showed that fluctuations in the wall temperatures exceed 5 °C in more than 50% of the tests and reached differences as high as 23 °C. The wall temperature instabilities in CFB indicate that one temperature may be inaccurate and that by including time as a variable a better understanding of the behaviour at this scale may be revealed

1. Introduction

High power densities of current and future power systems and high performance electronics have created a continuing need for novel thermal management. Historically, these problems emerged as transistor sizes decreased and the density of transistors increased. Each transistor, now closely packed, leads to an ever increasing heat flux that must be removed, or devices will overheat. Within the large arena of solutions to this problem is some very promising research utilizing phase change devices, such as loop heat pipes and vapor chambers. [1-3]. These direct phase change liquid cooling schemes have been a leading topic of research for many years, including a large body of work focused on pool boiling with different surfaces. The goal of most pool boiling work is to raise the critical heat flux (CHF) as high as possible [4]. This critical heat flux marks the point where devices can no longer remove additional power and the turning point where the textured surface overheats. Recent work in this area has pushed the CHF higher than ever thought possible [5]. With this great progress, it is time for a shift to be made to translate these surfaces into phase change devices.

One proposed solution is to start testing these surfaces in more realistic conditions by moving away from pool boiling and into convective flow boiling (CFB). Testing patterned surfaces with both evaporation and flow is more realistic to looping systems, and will hopefully help with the long-term goal of integrating these surfaces into systems with circulating fluid. Researchers have tried for many years in other CFB applications to gain insight by using correlations from large scale systems [6,7]. These correlations have been useful when trying to get a general sense of how a device will work, but there are many anomalies between large and micro scale flow and heat transfer patterns [3].

One large issue between conventional large systems and MEMS based systems has to do with the stability of micro-scale flow behavior. Studies that have explored convective flow in pin fins defer the issues associated with instabilities by taking averages or measurements over short time periods. The work presented here aims to begin showing some instabilities that arise when temperature is measured in these devices over an extended period of time.

2. Background

Loop heat pipes (LHPs) are a passive phase change thermal management device similar to heat pipes. In these devices, evaporation and the subsequent transfer of latent heat is used to efficiently remove heat from a critical area of a device [8]. The looping fluid is driven by capillary forces and thus the fluid flow rates are very low. The efficiency of the LHP is balanced between three areas: proper condensation, wicking ability, and efficient evaporation. The third challenge is addressed in this paper through the implementation of an experiment to examine thin-film evaporation.

This idea of utilizing thin-film evaporation stems from a desire to avoid macro to micro correlations and begin building surfaces solely for use on the micro scale. With this in mind, the surfaces have been based on a theory of thin film evaporation, called interline or sub region evaporation, where nucleation bubbles are avoided [9]. In this case, a film is created that allows liquid to transition straight from liquid to vapor. Promising work from Purdue showed that between 66% and 87% of all heat transfer in an evaporation system occurs in a very small region [10]. This work drove the focus on designing small features that create this thin film during convective flow boiling. To create this behavior, a model was used to influence the height to diameter ratio. The final chosen ratio was 2.5 with a height to feature spacing ratio of 2. The choice of these ratios has to do with minimizing friction and decreasing the possibility of pressure instabilities due to meniscus recession [3, 11]. This work lead to the development of several pin fin surfaces that were tested using a new method that is described in this paper.

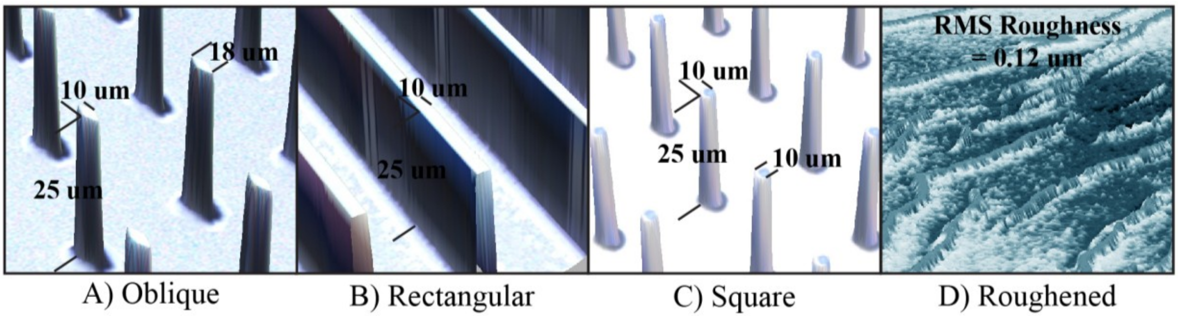

Figure 1. A 3D laser confocal microscope image of the four surface structures tested in this work.

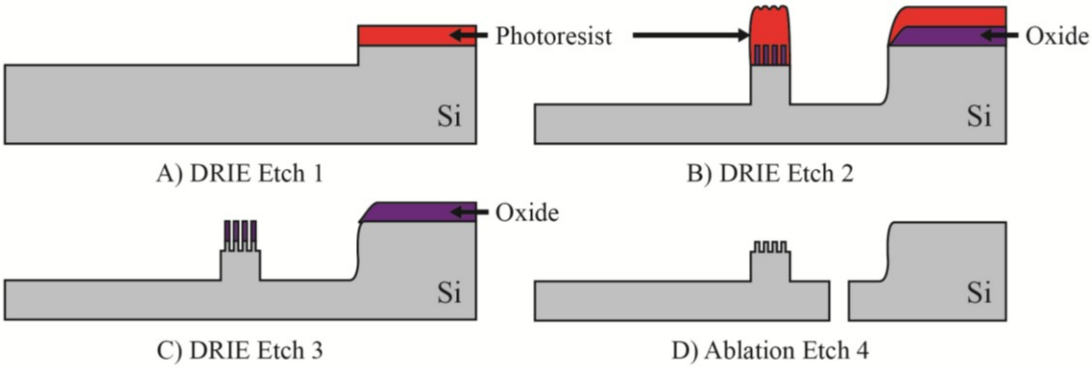

Figure 2. A simple schematic of the fabrication process used to make the tested devices.

3. Fabrication and Overview of the Pin Fins and Roughened Surfaces

The chosen pin fin structures were, oblique, rectangular, and square shaped pins, with the fourth surface blank, but roughened by deep reactive ion etching (DRIE). The size, shape and layout of the final surface are shown in figure 1. The roughened surface has an RMS roughness of 0.12 ± 0.02 µm with a maximum valley to peak distance of 1.25 ± 0.02 µm.

The pin fin surfaces were fabricated in a one sided, n-type, silicon wafer using a three mask process. The final structure has four different depths created using two masking materials, oxide and photoresist, and a laser ablation system. In order to create these different depths the wafer was processed using standard CMOS fabrication techniques including photolithography, reactive ion etching (RIE) for selective oxide removal and deep reactive ion etching (DRIE) for selective silicon removal. The general concept of masking allows patterns to be created by photolithography and then any part of the wafer that is uncovered by the masking material is removed during the etching process (see figure 2, step A).

In order to save time and avoid a long DRIE etch, all the way through the wafer, a laser ablation method was used to cut 2 mm holes in the silicon wafer. The laser system used a Universal PLS 6MW laser with a multi-wave 1.06 µm , 30 W fiber laser. This method turned out to be very effective. It allowed for ten holes to be drilled in about 20 minutes, drastically reducing the time required for DRIE etching. One downside of this process was the rough edges of the through holes. However, the holes were still effective. Once the through holes were created the wafer was cleaned and a 1.1 mm thick glass wafer was anodically bonded to the wafer to seal the device.

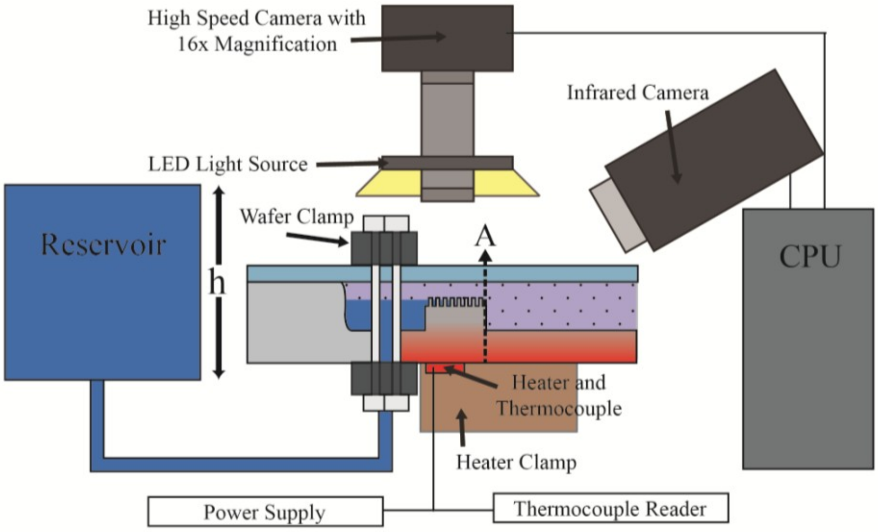

Figure 3. A schematic of the testing set up for the evaporation tests. The IR camera measurements were recorded at the point labeled A, approximately 3mm away from the hottest point.

4. Experimental Set Up and Procedure

Figure 3, shows a schematic of the experimental test set-up. The major equipment used was a high speed camera, an infrared camera, a high accuracy thermocouple reader, a power supply and a high temperature heater. For testing, the glass capped chip is placed into the small wafer clamp shown in figure 3. One of these small clamps was placed on each of the four tested chips. These clamps could then be easily moved in and out of the larger Teflon heater clamp, allowing for all of the chips to be tested without having to move any of the larger equipment. The heater clamp was anchored to a larger structure and held the heater and thermocouple. These were attached to a thermocouple reader and power supply. The fluid was supplied from a hydrostatic reservoir, where the height of the reservoir supplied a pressure that set the flow rate. The pressure was calculated using the following equation.

$$P = \rho g H \quad (1)$$

To begin testing, the flow from the reservoir was started, by opening the valve, and the chips were flooded. The IR camera began recording data and then the power supply that was attached to the heater was programmed and switched on to begin the evaporation process. The location of the temperature measurement was at the end of the surfaces indicated on figure 3 with the letter A.

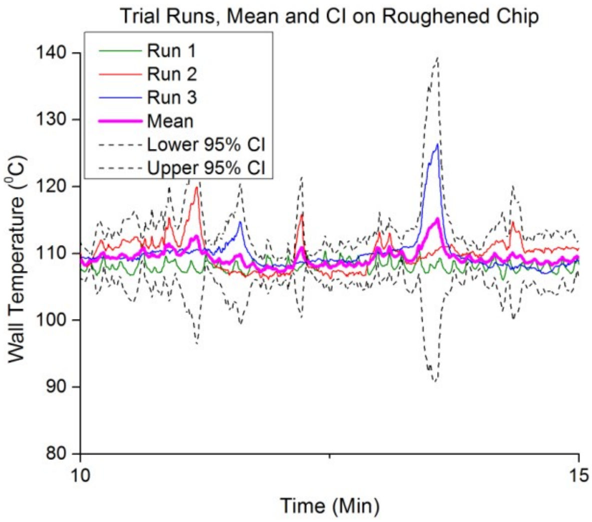

Figure 4. Raw temperature data for roughened chip at 40W/cm^2 and 1150 Pa.

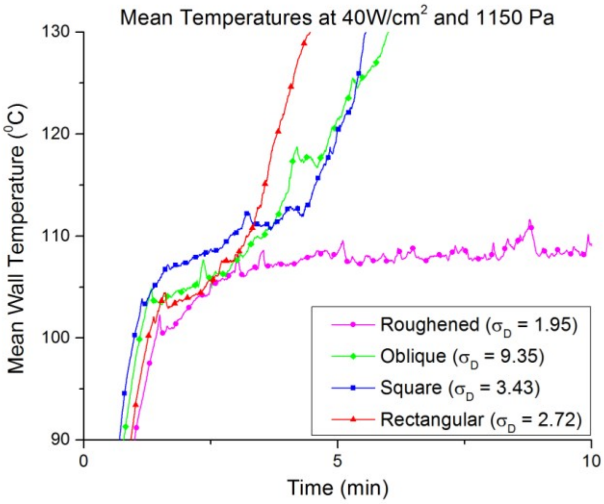

Figure 5. Mean temperature data for all four surfaces at 40W/cm^2 and 1150 Pa.

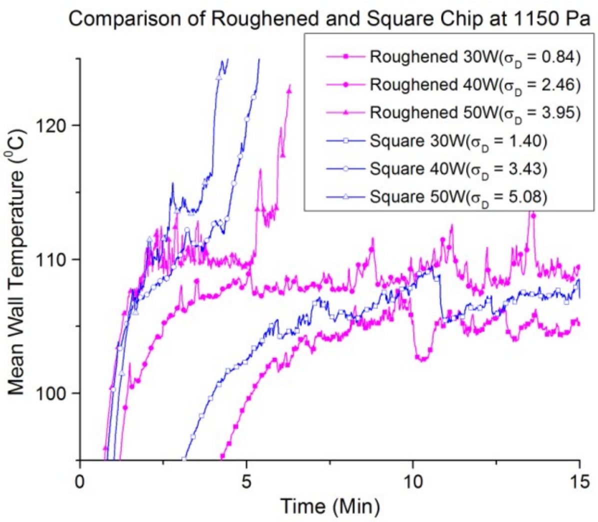

Figure 6. Mean temperature data for the square and roughened chips at three power densities.

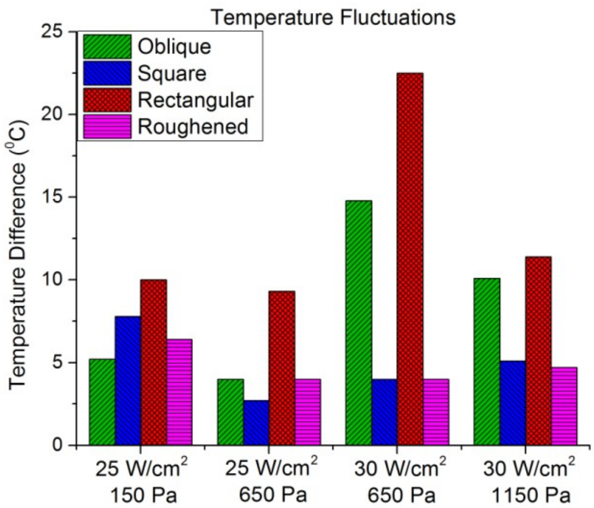

Figure 7. Temperature fluctuations above the mean wall temperature for all of the devices.

5. Results and Discussion

The results follow a path from raw data to a final comparison of the two most promising surfaces. Figure 4 shows three individual trials that were run for 60 minutes each (although the image only shows a 5 minute section). The complete data set includes the device heating up and many peaks. By zooming into a section, more important aspects become increasingly visible. Here, the mean is visible as well as the upper and lower bounds of the confidence interval. Within the confidence interval, areas with small deviations have closer confidence intervals indicating better data. Figure 5 shows the average temperatures of all four chips at 40 W/cm^2 and 1150 Pa. This is the highest power and pressure where all of the chips were tested. The oblique and rectangular chips were not tested at 50

W/cm^2, because they dried out quickly, and it was assumed that at a higher power they would also dry out. These two chips also had a lot of temperature fluctuations in lower power tests, indicating that these chips were not performing well. Figure 5 also shows the square chip drying out quickly, but earlier tests with small fluctuations showed that this was the second most promising chip. Figure 6 is the final analysis, where average temperatures for the square and roughened chip are compared at 1150 Pa and three different fluxes: 30, 40 and 50 W/cm^2. This data shows that the roughened chip survived higher power densities for longer periods of time with very good stability.

This data can further be manipulated to detail the maximum fluctuations at the measurement spot, (figure 3). Fluctuations were calculated by subtracting the maximum peak temperature from the average wall temperature over the entire test. The fluctuations are shown for the lower power and lower pressure potential tests in figure 7. These lower tests are shown because the fluctuations do not include dry out or device failure. By definition, fluctuations include the devices reaching high temperatures from which the chips recovered. Recovery means that the temperatures went back down to a temperature close to the mean. The higher power and pressure tests resulted in chip failure that makes it difficult to calculate the wall fluctuations.

An advantage of taking time dependent data is the availability of these fluctuation results. It is clear from the data that wall temperatures do not stay constant, as fluctuations of 5 or more degrees occurred in more than 50% of the tests. From this information, it seems logical that temperature data taken over short time periods may be missing profile details. It is also possible that data taken during a high fluctuation could reveal different wall temperatures than an average over a longer time frame. For this reason, a longer time test may be valuable for convective flow boiling tests on pin fin surfaces.

6. Conclusion

A testing procedure and results for convective flow boiling over roughened pin fin surfaces are presented. The results show that, of four tested pin fin structures, a roughened surface withstood higher power densities for longer time periods than the other structures under the presented conditions. Temperature fluctuations were shown as a possible indication of device and boiling behavior. However, the real conclusion of the temperature fluctuations was that valuable information on the stability of the flow over a surface is indicated when a time variable is added to the study. These results suggest that further exploration into this testing procedure and apparatus could yield better models of flow boiling in pin fins and reveal additional correlations.

References

[1] Krishnan S, Garimella S V, Chrysler G M and Mahajan R V 2007 *IEEE Transactions on Advanced Packaging* **30** 462-474
[2] Pastukhov V, Maidanik Y, Vershinin C and Korukov M 2003 *Applied Thermal Engineering* **23** 1125–1135
[3] Koşar A and Yoav P 2006 *Int. J. Heat and Mass Transfer* **49** 3142-3155
[4] Honda H and Wei J J 2004 *Experimental Thermal and Fluid Science* **28** 159-169
[5] Chu K, Enright R, and Wang E 2012 *Applied Physics Letters*, 241603-1 - 241603-4.
[6] Peles Y, Koşar A, Mishra C, Kuo C J and Schneider B 2005 *Int. J. Heat and Mass Transfer* **48** 3615-3627
[7] Arana L R, Schaevitz S B, Franz A J, Schmidt M A and Jensen K F 2003 *J. Microelectromech. Syst.* **12** 600-612
[8] Dhillion N S, Hogue C, Cheng J C and Pisano A P 2011 *Proceedings of PowerMEMS* (Seoul, Republic of Korea)
[9] Wang H, Garimella S V and Murthy J Y 2007 *Int. J. Heat and Mass Transfer* **50** 3933-3942
[10] Dhavaleswarapu H K, Garimella S and Murthy J Y 2009 *Birck and NCN Publication* Paper **384.**
[11] Nilson R H, Tchikanda S W, Griffiths S K and artinez M J 2006 *Int. J. Heat and Mass Transfer* **49** 1603-1618